

## Multi-label classification of frog species via deep learning

Jie Xie\*, Rui Zeng<sup>§</sup>, Changliang Xu<sup>‡</sup>, Jinglan Zhang<sup>§</sup> and Paul Roe<sup>§</sup>

\*Department of Electrical and Computer Engineering, University of Waterloo

Email: xiej8734@gmail.com

<sup>‡</sup>College of Automation Engineering, Nanjing University of Aeronautics and Astronautics,

Email: xuchangliang@nuaa.edu.au

<sup>§</sup> Science and Engineering Faculty, Queensland University of Technology,

Email: r5.zeng, jinglan.zhang, p.roe@qut.edu.au

**Abstract**—Acoustic classification of frogs has received increasing attention for its promising application in ecological studies. Various studies have been proposed for classifying frog species, but most recordings are assumed to have only a single species. In this study, a method to classify multiple frog species in an audio clip is presented. To be specific, continuous frog recordings are first cropped into audio clips (10 seconds). Then, various time-frequency representations are generated for each 10-s recording. Next, instead of using traditional hand-crafted features, various features are extracted using pre-trained networks using three time-frequency representations: Fast-Fourier spectrogram, Constant-Q transform spectrogram, and Gammatone-like spectrogram. Finally, a binary relevance based multi-label classification approach is proposed to classify simultaneously vocalizing frog species with our proposed features. Our proposed method is verified using eight frog species widely distributed in Queensland, Australia. The results show that the proposed features extracted via pre-trained networks can achieve better classification performance when compared to hand-crafted features for classifying multiple simultaneously vocalizing species.

**Keywords**—soundscape ecology, frog call classification; multi-label learning; deep learning

### I. INTRODUCTION

As a widely distributed amphibian species, frogs are an integral part of the food web, and are often regarded as a valuable indicator species for environmental health [1]. Although frogs are very important, rapid decline in frog populations has been spotted worldwide. Reasons for this decline can be summarized as habitat loss, invasive species, climate change. To monitor the change of frog population and optimize its protection policy, it is becoming ever more important to gain insights about frogs and the environment. Compared to traditional methods that require ecologists to enter the fields frequently for biodiversity data collection, an acoustic sensor provides a way to collect data over larger spatial and temporal scales [2]. Since large volumes of acoustic data can be generated by an acoustic sensor, enabling automatic methods to study collected data is in high demand.

In previous studies, various feature sets and classifiers have been explored for frog call classification. Lee et al. [3] introduced a recognition method based on the analysis of

spectrogram to detect each syllable. Mel-frequency cepstral coefficients features (MFCCs) of each frame were defined as features, and linear discriminant analysis was used for classifying 30 kinds of frog calls and 19 kinds of cricket calls. Huang et al. [4] calculated spectral centroid, signal bandwidth and threshold crossing rate from segmented syllables. Then, k nearest neighbor (k-NN) and support vector machine (SVM) classifiers were combined with those features to classify frog calls. Dayou et al. [5] developed a hybrid spectral-entropy method to recognize frog calls. Spectral centroid, Shannon entropy, Renyi entropy were combined as inputs to a k-NN classifier for recognition. Chen et al [6] proposed to firstly use syllable length for pre-classification. Then, a multi-stage average spectrum was extracted to further classify frog species based on distance calculation. Recently, Xie et al. [7] used a large feature set to classify frog species with five classifiers. [8] presented a system for semi-automated segmentation of anuran calls and classification of 17 anurans species. However, recordings used in those previous studies often have a high signal-to-noise ratio (SNR), and each recording is assumed to include a single species.

In contrast, recordings used in this study have a low SNR and contain many overlapping animal vocal activities, including frogs, birds, crickets. To address those challenges, multi-label learning is introduced to classify simultaneously vocalizing frog species in low SNR recordings. Various methods have been proposed to classify simultaneously vocalizing birds [9] and frogs [10]. However, hand-crafted features are used in those studies, which are highly affected by the segmentation process. Compared to hand-crafted features, recent use of deep learnings has achieved state-of-the-art accuracy in frog call classification [11], [12], but all recordings used are assumed to have a single species.

After changing one-dimensional audio data into its two-dimensional representation, researchers can perform quick visual analysis. Inspired by this visual inspection practice in audio analysis, it has attracted increasing attention to apply image processing techniques to analyze animal calls automatically [13]. In this study, we use a deep learning algorithm to extract features, where pre-trained networks

based on images are used. After splitting continuous recordings into 10-s audio clips, we translate each recording into its time-frequency representation. Then, acoustic features are directly extracted from the time-frequency representation with a pre-trained network. Different from hand-crafted features, we do not need to segment recordings into individual events as previous studies [9], [10], which can increase the robustness of our classification model. To classify simultaneously vocalizing frog species, a binary relevance based multi-label classification approach is used. Eight frog species, which are widely distributed in Queensland, Australia, are selected for the experiment.

The rest of this paper is organized as follows: In section II, we describe the method for frog call classification, which includes data description, feature extraction, and classification. Section III reports experimental results. Section IV presents conclusion and future work.

## II. METHODS

Our frog call classification method consists of four steps: data description, signal pre-processing, feature extraction, and classification (Fig. 1). Detailed information of each step is shown in following sections.

### A. Data description

Digital recordings in this study were obtained with a battery-powered, weatherproof Song Meter (SM2) box<sup>1</sup>. Recordings were two-channel, sampled at 22.05 kHz and saved in WAC4 format. A representative sample of 342 10-s recordings was selected to train and evaluate our proposed algorithm for classifying simultaneously vocalizing frog species in a recording. All those examples were collected between 02/2014 to 03/2014, since it is breeding season for frogs with high calling activity. All the species that are presented in each 10-s recording were manually labeled by an ecologist who is a frog expert. There are totally eight frog species in the recordings, which are widely distributed in Queensland Australia for analysis.

Table I: Scientific name, code and common name of eight frog species used in this study.

Scientific name	Code	Common name
Rhinella marina	RMA	Canetoad
Cyclorana novaehollandiae	CNE	New Holland frog
Limnodynastes terraereginae	LTE	Northern banjo frog
Litoria fallax	LFX	Eastern dwarf tree frog
Litoria nasuta	LNA	Striped rocket frog
Litoria rothii	LRI	Roth's tree frog
Litoria rubella	LRA	Desert tree frog
Uperoleia mimula	UMA	Mimic Toadlet

<sup>1</sup><https://www.wildlifeacoustics.com>

### B. Signal pre-processing

All the recordings were re-sampled at 16 kHz and mixed to mono. Since features are directly calculated by applying deep learning techniques to recordings' time-frequency representations. Three time-frequency representations are tested in this study: fast-Fourier transform spectrogram, constant-Q transform spectrogram, and Gammatone-like spectrogram.

Fast-Fourier transform (FFT) spectrogram is generated by applying short-time Fourier transform (STFT) to each recording. Specifically, each recording was divided into frames of 32 ms with 50 % frame overlap. A fast Fourier transform was then performed on each frame with a Hanning window, which yielded amplitude values for 256 frequency bins, each spanning 31.25 Hz. The final decibel values ( $S$ ) were generated using

$$S_{tf} = 20 * \log_{10} A_{tf} \quad (1)$$

where  $t = 0, \dots, T - 1$ ,  $f = 0, \dots, F - 1$ ,  $t$  and  $f$  represent frequency bin and time index,  $T$  and  $F$  are 256 frequency bins and 625 frames,  $A$  is the amplitude value.

Constant-Q transform spectrogram is generated by applying constant-Q transform to the signal. Compared to STFT, this transform provides a frequency analysis on a log-scale which makes it more adapted to sound with harmonic structures. Here we use 48 filters per octave with lowest and high frequency as 50 Hz and 8000 Hz.

Gammatone-like spectrogram is constructed by first calculating a conventional, fixed-bandwidth spectrogram, then combining the fine frequency resolution of the FFT-based spectra into the coarser, smoother Gammatone responses via a weighting function. Here, each recording was passed through a 64 channel gammatone auditory model filterbank, with lowest and highest frequency as 50 Hz and 8000 Hz. The outputs of each band have their energy integrated over windows of 25 ms with 60% overlap.

Before using pre-trained networks for feature extraction, all time-frequency representations are normalized as follows.

$$S = \frac{S - \min(S)}{\max(S) - \min(S)} \quad (2)$$

where  $S$  denotes a type of time-frequency representation.

### C. Feature extraction

Different from [11], we use a deep learning algorithm as a feature extractor. In [12], a pre-trained network is found to achieve higher classification accuracy than training a new network. Also, there are only 342 10-s recordings for the experiment, which are not enough for training. Here, we directly use a pre-trained network to extract features by removing the vectors from one of the final fully connected layers. Multiple different networks, which are trained on ImageNet with different architecture, are used: AlexNet, CaffeNet, and VGG1 since those networks have shown success in single-label classification of frog species [12].

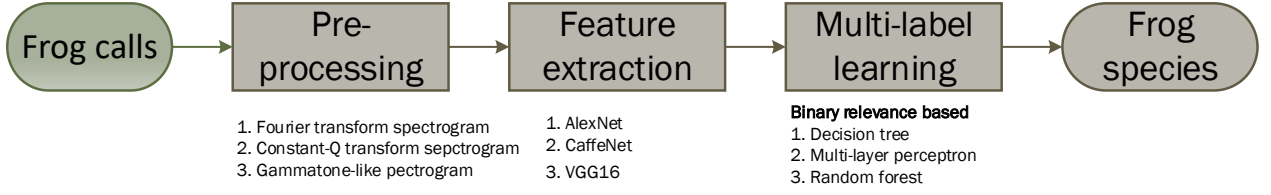


Figure 1: Flowchart of our frog call classification system using pre-trained deep networks and multi-label learning. Three time-frequency representations and three pre-trained networks and three types of classifiers are used for the classification.

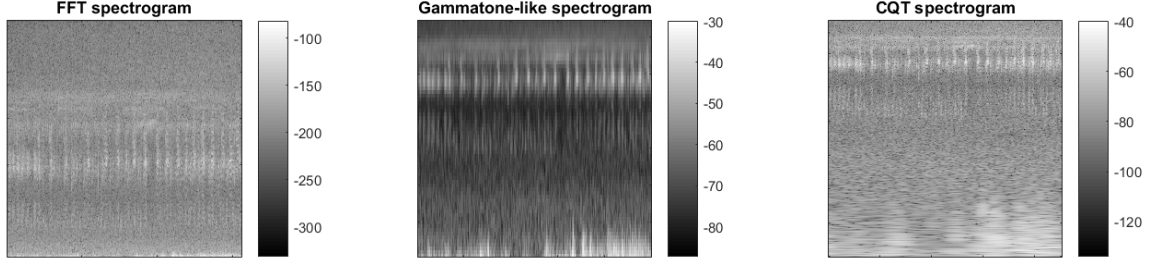


Figure 2: Spectrogram comparison using three time-frequency representations. Here, x-axis and y-axis denote the time and frequency index, respectively.

AlexNet [14] was trained on the 1.3 million images in the LSVRC-2010 ImageNet training set for 1000 categories classification. AlexNet consists of five convolutional layers, three fully connected (fc) layers. The architecture and parameters of AlexNet model for frog call classification are summarized in Fig. 3.

CaffeNet [15] has a similar architecture as AlexNet. The difference is that CaffeNet was trained with data that was augmented differently and the pooling and normalization layers were switched. The architecture and parameters of CaffeNet model for frog call classification are summarized in Fig. 4.

VGG16 [16] was trained on a subset of the ImageNet database, which was used in the ImageNet Large-Scale Visual Recognition Challenge (ILSVRC). The architecture and parameters of VGG16 model for frog call classification are summarized in Fig. 5.

For both AlexNet and CaffeNet, the input image size are  $227 \times 227$ . The input image size of VGG16 is  $224 \times 224$ . However, the sizes of three time-frequency representations are different from each other. To use those pre-trained networks, all time-frequency representations are resized to the corresponded net size. After resizing, the structure of the 2D representation can be well kept for the subsequent analysis. Fig. 6 shows a comparison before and after resizing.

#### D. Multi-label learning

In this study, a binary relevance (BR) based multi-label learning is used for its scalability and flexibility [17]. The principle of the BR method is to solve a multi-label classification problem using multiple binary classifiers. Considering the relevance of each training sample to  $y_j$ , binary relevance firstly construct a binary training set for the  $j$ -th class label  $y_j$  as follows:

$$D_j = (x_i, \phi(Y_i, y_j)) | 1 \leq i \leq m \quad (3)$$

where  $\phi(Y_i, y_j)$  is the  $j$ -th class label indicator which is +1 for  $y_j$  belongs to  $Y_i$ , and -1 for  $y_j$  not belong to  $Y_i$ .

Based on this strategy, binary learning algorithms can be used for inducing a binary classifier. Therefore, for any multi-label training example  $(x_i, Y_i)$ ,  $q$  binary classifiers will be used to learn a single instance  $x_i$ . For relevant label  $y_j \in Y_i$ ,  $x_i$  is regarded as one positive instance in inducing  $g_j(\cdot)$ . As for irrelevant label  $y_k \in \hat{Y}_i$ ,  $x_i$  is regarded as one negative instance.

For predicting, the associated label set  $Y$  is obtained by querying labeling relevance on each individual binary classifier and combing relevant labels.

$$Y = \{y_j | g_j(x) > 0, 1 \leq j \leq q\} \quad (4)$$

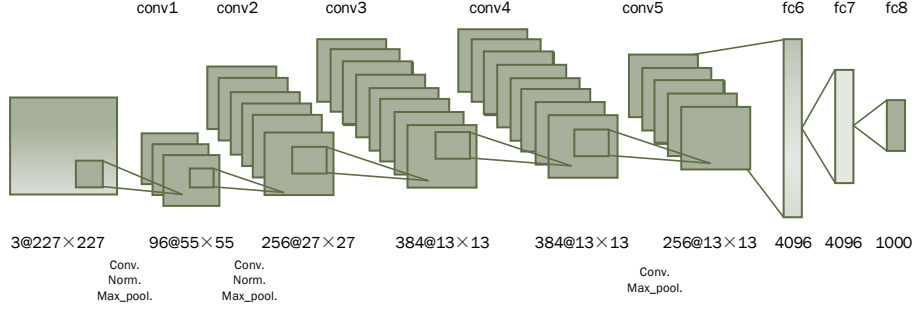


Figure 3: The example architecture of AlexNet model for frog feature extraction.

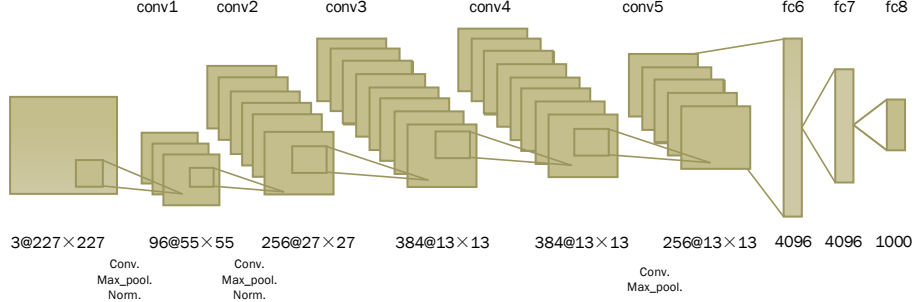


Figure 4: The example architecture of CaffeNet model for frog feature extraction.

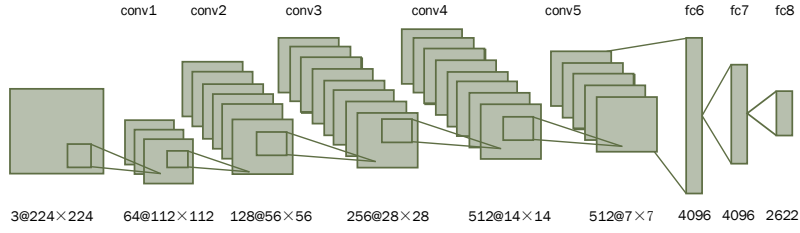


Figure 5: The example architecture of VGG16 model for frog feature extraction.

Since the predicted label set  $Y$  would be empty when all binary classifiers yield negative outputs, a following *T-Criterion* rule is used.

$$Y = \{y_j | g_j(x) > 0, 1 \leq j \leq q\} \cup \{y_j^* | j^* = \arg\max_{1 \leq j \leq q} g_j(x)\} \quad (5)$$

The use of *T-Criterion* rule use the class label with greatest as output when none of the binary classifiers yield positive predictions.

Similar to our previous work [18], three classic single-label learning algorithms are used in this study: decision tree (DT), and k-nearest neighbour (k-NN), and random forest (RF). For each classifier, a grid search is conducted

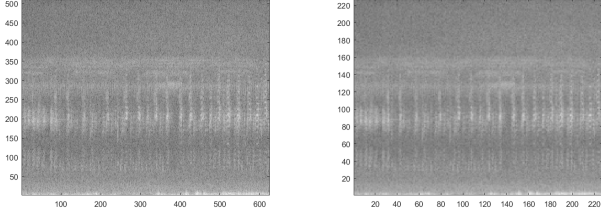
to optimize classification results. To evaluate the multi-label classification model, a tagged representative sample of 342 10-s recordings is used with 5-fold cross-validation.

#### E. Evaluation metrics

Three evaluation metrics are used: Hamming loss, accuracy, and subset accuracy [19].

##### (1) Hamming loss

Hamming loss is defined as the fraction of labels that are incorrectly predicted for an instance and the normalised Hamming loss which is normalized over instances is reported. This metric is defined as



(a) Before resizing

(b) After resizing

Figure 6: Time-frequency representations before and after resizing. The x-axis denotes the time index, y-axis is the frequency index. Here a brighter pixel represents a higher amplitude value.

$$hammingLoss = \frac{1}{N} \sum_{i=1}^N \frac{1}{Q} |h(x_i) \Delta y_i| \quad (6)$$

where  $\Delta$  denotes the symmetric difference between two instances,  $N$  is the number of instances and  $Q$  is the total number of possible labels.  $y_i$  denotes the ground truth of instance  $x_i$ , and  $h(x_i)$  denotes the predictions for the same instance.

To better interpret these results, a baseline for Hamming loss is obtained by considering a non-informative classifier that cannot predict any accuracy labels [9]. The value of Hamming loss is then calculated as follows:

$$HammingLossBaseLine = \frac{c * n}{\sum_{i=1}^n y_i} \quad (7)$$

where  $c$  is the number of frog species,  $n$  is the number of recordings.

#### (2) Accuracy

Accuracy for a single instance  $x_i$  is defined by the Jaccard similarity coefficients between the ground truth  $y_i$  and the prediction  $h(x_i)$ . Accuracy is micro-averaged across all examples:

$$accuracy = \frac{1}{N} \sum_{i=1}^N \frac{|h(x_i) \cap y_i|}{|h(x_i) \cup y_i|} \quad (8)$$

#### (3) Subset accuracy

Subset accuracy is defined as follows:

$$subsetAccuracy = \frac{1}{N} \sum_{i=1}^N I(h(x_i) = y_i) \quad (9)$$

where  $I(true) = 1$  and  $I(false) = 0$ . This is a very strict evaluation measure as it requires the predicted set of labels to be an exact match of the true set of labels.

Values for hamming loss, accuracy, and subset accuracy range from zero to one. For hamming loss, zero denotes the perfect result, and one means the wrong prediction of all

labels over every instance, whereas for accuracy and subset accuracy, the values have complete opposite meanings.

### III. EXPERIMENTAL RESULTS AND DISCUSSIONS

In this experiment, three time-frequency representations are first compared using AlexNet. Here, features are extracted from multiple fully connected layers, including layer  $fc6$ ,  $fc7$ , and  $fc8$ . As for the classification, a BR based multiple learning is used with three classic single-label learning algorithms as binary classifiers: DT, k-NN, and RF. Default parameters of Meka are used and summarized in Table II for the classification.

Table II: Summarized parameters for three standard classifiers.

Standard classifiers	Parameters
k-NN	K = 1 and nearest neighbor search
DT	Confident factor = 0.25 Minimum number of instance per leaf = 2
Random Forest	No. of Trees = 100 No. of exclusion slots = 1

#### A. Comparison of three time-frequency representations using three layers and DT

Classification results of AlexNet are shown in Table III with DT. Compared to FFT spectrogram and CQT spectrogram, gamma spectrogram using layer  $fc7$  achieves the best Hamming loss and subset accuracy. According to Fig. 2, gamma spectrogram is the time-frequency representation with a highest resolution, which is in accordance to the classification result. Therefore, gamma spectrogram is selected for the subsequent analysis.

Table III: Classification results using AlexNet. The best value of each evaluation metric is in bold. Here  $\downarrow$  means that a higher value implies a better performance, but  $\uparrow$  has a completely opposite meaning.

Layer	TF representation	Hamming loss $\downarrow$	Accuracy $\uparrow$	Subset accuracy $\uparrow$
fc6	FFT spectrogram	0.150	0.589	<b>0.310</b>
fc6	CQT spectrogram	0.151	0.585	0.301
fc6	Gamma spectrogram	0.147	0.588	<b>0.310</b>
fc7	FFT spectrogram	0.156	0.576	0.295
fc7	CQT spectrogram	0.160	0.571	0.289
fc7	Gamma spectrogram	<b>0.138</b>	0.591	<b>0.310</b>
fc8	FFT spectrogram	0.149	<b>0.598</b>	0.301
fc8	CQT spectrogram	0.152	0.584	0.289
fc8	Gamma spectrogram	0.145	0.584	0.284

#### B. Comparison of three networks using three basic single-label learning algorithms

In this part, gammatone-like spectrogram with  $fc7$  layer is used for various networks and three classifiers due to its best performance in Table III. Table IV shows that AlexNet with RF and VGG16 with k-NN are two best classification systems. Among three classifiers, the classification performance of DT is the worst. Compared to AlexNet and VGG16, CaffeNet is the worst, which is in consistent with [12].

Table IV: Classification results using three pre-trained networks and three standard classifiers.

Net	Classifier	Hamming loss ↓	Accuracy ↑	Subset accuracy ↑
AlexNet	DT	0.138	0.591	0.310
AlexNet	k-NN	0.117	0.691	0.444
AlexNet	RF	<b>0.097</b>	0.692	0.477
CaffeNet	DT	0.160	0.572	0.298
CaffeNet	k-NN	0.133	0.651	0.418
CaffeNet	RF	0.111	0.647	0.412
VGG16	DT	0.151	0.597	0.319
VGG16	k-NN	0.109	<b>0.711</b>	<b>0.482</b>
VGG16	RF	0.099	0.679	0.462

### C. Comparison with hand-crafted features and baseline

We also compare the performance between hand-crafted features and deep learning based features using the RF. In our previous studies, the best classification results for Hamming loss are 0.131 and 0.182, which are obtained using multi-label learning and multiple-instance multiple-label learning. The hand-crafted features used for multi-label learning are wavelet-based cepstral coefficients and linear predictive coefficients. However, this kind of global features will cause the information loss in time domain. Features extracted from segmented frog syllables using acoustic event detection are highly affected by the segmentation results. The segmentation process is sensitive to the background noise, which makes the classification results sensitive.

## IV. CONCLUSIONS AND FUTURE WORK

In this study, we explore pre-trained networks for extracting acoustic features to classify multiple simultaneously vocalizing frog calls. Continuous recordings are first segmented into 10-s audio clips. Then, three types of time-frequency representations are used for extracting features with three pre-trained networks. Finally, a binary relevance based multiple-label classification algorithm is used to classify frog species with three single-label learning algorithms: DT, k-NN, and RF. Experimental results on 342 recordings of eight frog species are promising with hamming loss, accuracy and subset accuracy as 0.109, 0.711, and 0.482, respectively. Compared to hand-crafted features, features extracted using deep learning can achieve a better classification performance.

The size of recordings used in this study is quite small, future work will include a larger dataset for the experiment. Also, data augmentation and fine tuning of networks have shown potential improvement in the final classification results, which is worthwhile testing. Currently, the multi-label method used is binary relevance. Other methods, such as the random k-labelsets, classifier chains, need to be investigated.

### ACKNOWLEDGMENT

The authors would like to thank the Eco-acoustic group of Queensland University of Technology and James Cook University for providing the data. Any opinions, findings and conclusions or recommendations expressed in this material

are those of the authors and do not necessarily reflect the views of QUT and JCU.

## REFERENCES

- [1] S. Böll, B. Schmidt, M. Veith, N. Wagner, D. Rödder, C. Weinmann, T. Kirschey, and S. Loetters, "Amphibians as indicators of changes in aquatic and terrestrial ecosystems following gm crop cultivation: a monitoring guideline," *BioRisk*, vol. 8, p. 39, 2013.
- [2] J. Wimmer, M. Towsey, B. Planitz, I. Williamson, and P. Roe, "Analysing environmental acoustic data through collaboration and automation," *Future Generation Computer Systems*, vol. 29, no. 2, pp. 560–568, February 2013.
- [3] C.-H. Lee, C.-H. Chou, C.-C. Han, and R.-Z. Huang, "Automatic recognition of animal vocalizations using averaged mfcc and linear discriminant analysis," *Pattern Recognition Letters*, vol. 27, no. 2, pp. 93–101, 2006.
- [4] C.-J. Huang, Y.-J. Yang, D.-X. Yang, and Y.-J. Chen, "Frog classification using machine learning techniques," *Expert Systems with Applications*, vol. 36, no. 2, pp. 3737–3743, 2009.
- [5] N. C. Han, S. V. Muniandy, and J. Dayou, "Acoustic classification of australian anurans based on hybrid spectral-entropy approach," *Applied Acoustics*, vol. 72, no. 9, pp. 639–645, 2011.
- [6] W.-P. Chen, S.-S. Chen, C.-C. Lin, Y.-Z. Chen, and W.-C. Lin, "Automatic recognition of frog calls using a multi-stage average spectrum," *Computers & Mathematics with Applications*, vol. 64, no. 5, pp. 1270–1281, 2012.
- [7] J. Xie, M. Towsey, J. Zhang, and P. Roe, "Acoustic classification of australian frogs based on enhanced features and machine learning algorithms," *Applied Acoustics*, vol. 113, pp. 193–201, 2016.
- [8] J. B. Alonso, J. Cabrera, R. Shyamnani, C. M. Travieso, F. Bolaños, A. García, A. Villegas, and M. Wainwright, "Automatic anuran identification using noise removal and audio activity detection," *Expert Systems with Applications*, vol. 72, pp. 83–92, 2017.
- [9] F. Briggs, B. Lakshminarayanan, L. Neal, X. Z. Fern, R. Raich, S. J. Hadley, A. S. Hadley, and M. G. Betts, "Acoustic classification of multiple simultaneous bird species: A multi-instance multi-label approach," *The Journal of the Acoustical Society of America*, vol. 131, no. 6, pp. 4640–4650, 2012.
- [10] J. Xie, M. Towsey, L. Zhang, K. Yasumiba, L. Schwarzkopf, J. Zhang, and P. Roe, "Multiple-instance multiple-label learning for the classification of frog calls with acoustic event detection," in *International Conference on Image and Signal Processing*. Springer, 2016, pp. 222–230.
- [11] J. Colonna, T. Peet, C. A. Ferreira, A. M. Jorge, E. F. Gomes, and J. Gama, "Automatic classification of anuran sounds using convolutional neural networks," in *Proceedings of the Ninth International C\* Conference on Computer Science & Software Engineering*. ACM, 2016, pp. 73–78.

- [12] S. M. S. M. B. E. R. Julia Strout, Bryce Rogan, "Anuran call classification with deep learning," *In: Proc. International Conference on Acoustics, Speech, and Signal Processing (ICASSP), New Orleans, USA,*, 2017.
- [13] J. Xie, M. Towsey, J. Zhang, X. Dong, and P. Roe, "Application of image processing techniques for frog call classification," in *Image Processing (ICIP), 2015 IEEE International Conference on.* IEEE, 2015, pp. 4190–4194.
- [14] A. Krizhevsky, I. Sutskever, and G. E. Hinton, "Imagenet classification with deep convolutional neural networks," in *Advances in neural information processing systems*, 2012, pp. 1097–1105.
- [15] Y. Jia, E. Shelhamer, J. Donahue, S. Karayev, J. Long, R. Girshick, S. Guadarrama, and T. Darrell, "Caffe: Convolutional architecture for fast feature embedding," in *Proceedings of the 22nd ACM international conference on Multimedia.* ACM, 2014, pp. 675–678.
- [16] O. Russakovsky, J. Deng, H. Su, J. Krause, S. Satheesh, S. Ma, Z. Huang, A. Karpathy, A. Khosla, M. Bernstein *et al.*, "Imagenet large scale visual recognition challenge," *International Journal of Computer Vision*, vol. 115, no. 3, pp. 211–252, 2015.
- [17] J. Read, B. Pfahringer, G. Holmes, and E. Frank, "Classifier chains for multi-label classification," *Machine learning*, vol. 85, no. 3, pp. 333–359, 2011.
- [18] L. Zhang, M. Towsey, J. Xie, J. Zhang, and P. Roe, "Using multi-label classification for acoustic pattern detection and assisting bird species surveys," *Applied Acoustics*, vol. 110, pp. 91–98, 2016.
- [19] G. Madjarov, D. Kocev, D. Gjorgjevikj, and S. Džeroski, "An extensive experimental comparison of methods for multi-label learning," *Pattern Recognition*, vol. 45, no. 9, pp. 3084–3104, 2012.